BULLETIN OF THE POLISH ACADEMY OF SCIENCES
TECHNICAL SCIENCES, Vol. 66, No. 5, 2018
DOI: 10.24425/124282

# Biomass fuel cell based distributed generation system for Sagar Island

P. KUMAR, P.S. SIKDER*, and N. PAL

Department of Electrical Engineering, Indian Institute of Technology (Indian School of Mines), Dhanbad, Jharkhand – 826 004, India

**Abstract.** Sustainable development of an area is highly dependable on reliable electrical energy supply. Due to the depletion of fossil fuels, and the contamination of the environment due to the generation of energy from primary energy sources, the energy sector is reforming and shifting towards a new era where renewable energy sources will become the primary focus of attention. At present, energy researchers and government organizations are interested in a distributed generation system using local renewable energy sources to electrify the rural areas situated far away from our mainland. Here, a biomass-based power supply system is being analyzed and compared with other potential power supply systems for Sagar Island. Sagar Island is the world's largest river-based island situated in the Sundarban deltaic complex, where the potential of biomass is huge due to the availability of natural forests, barren coastal areas full of weeds, agricultural by-products, cattle manure and waste materials from other sources. Here, an attempt has been made to provide sustainable electrical energy to the rural areas of the isolated Sagar Island for the sustainable development of the local people. This was done by means of using biomass and a fuel cell based electricity generation system.

**Key words:** biomass, fuel cell, distributed generation system, inverter, cost analysis.

## 1. Introduction

At present, the sustainable development of a nation is based on the utilization of electrical energy. India is a developing country, where *per capita* energy consumption is below the average energy consumption in other parts of the world and very much lower as compared to the world's most developed countries [1]. The *per capita* energy consumption only shows the overall picture of the nation's development but the actual picture of the development is different. The development index for rural areas is distinctly lower than for urban areas. Meanwhile, remotely located rural areas are in the worst condition. Due to unreliable electricity supply, their sustainable development remains in the primitive age. At present, most of the electricity is generated using fossil fuels. As such resources are being depleted in nature, it is difficult to further increase the generation of electricity to electrify the rural areas. Besides the problem related to the depletion of fossil fuels, the issue of environmental protection is also predominant. As fossil fuels contaminate our environment during the generation of electricity, further increase of generation of electricity destroys the environment's ecological balance . Under these circumstances, energy researchers pay most attention to the renewable energy sources allowing to generate electricity [2]. As grid connectivity in remote rural areas is not cost-effective, off-grid distributed generation systems, powered by the renewable energy sources, are the key to the sustainable development of such areas. In this present study, an off-grid distributed generation system for a remote rural area (Sagar Island) is constructed, ensuring lower environmental impact during the generation of electricity.

The Sundarban region is the world's largest delta, formed by the Ganges (Hugli in this region), Brahmaputra and Meghna. Sagar Island is located in the Sundarban areas of West Bengal. Like other parts of the Sundarban, it is characterized by mangrove swamps, waterways and small rivers, which are isolated from the mainland by the Indian Ocean and the Hugli River. Most of the Sundarban area is separated from the mainland by rivers and creeks, which renders establishing a grid-connected electricity supply system very difficult [3]. Due to insufficient electrical energy, sustainable development of Sagar Island is very poor and prospects for future development of that area also seem bleak.

So far studies have been conducted on solar energy or biomass gasification based electricity supply systems in the Sagar Island. The diesel generator acts as a standby unit to maintain reliability of the electricity [4]. Photovoltaic (PV) solutions with a grid-connected microgrid system are also studied on this island [5]. However, availability of the grid is concentrated in a little portion of the Sundarban area. So, the solar PV-based microgrid system is not feasible for the entire Sagar Island. Off-grid technology is much more effective in this situation. The PV diesel generator based hybrid system is also used here to electrify Sagar Island [6]. Yet the diesel generator connected system normally creates air pollution and is thus responsible for the changes in the island's biodiversity. On the other, due to seasonal variations, solar irradiance reduces drastically, which causes a decrease in electricity generation. To increase reliability of the electricity being generated, a battery-connected standalone system is used. Reliability of the power supply system is not up to the mark as the battery has its own limitations for storing the energy generated and it supplies it only for a limited time period. Recent studies

*e-mail: parthasarothi.sikder@gmail.com

Manuscript submitted 2017-09-20, revised 2018-02-06, initially accepted for publication 2018-03-01, published in October 2018.

show that production of different battery parts contaminates our environment by contaminating soil and water. One study also indicates that battery exhaust materials are also considered a pollutant. Hence, the application of batteries is not reliable as it pollutes the environment and damages the ecological balance where biodiversity is sensitive [7–8]. The availability of biomass energy is excellent on Sagar Island and it has a huge potential for the generation of electricity. Moreover, the availability of land and cultivation-related extract material along with human and cattle waste materials also show the huge potential for generation of biomass. Here, an attempt has been made to study the biomass fuel cell (FC) based power supply system for Sagar Island. In some developed countries the fuel cell based power supply system has already been launched successfully. For instance in Canada, as electricity production from hydropower is inexpensive. Meanwhile, the authorities of Japan produce hydrogen from low-cost electricity using the electrolyzer, and then transport the hydrogen thus generated to Japan to regenerate electricity [9]. The Norwegian energy company of Hydro has already set up a hydrogen-based power supply system municipality in Utsira, Norway, allied with the German wind turbine manufacturer of Enercon. The help of the Norwegian government has allowed to construct the hydrogen-based power supply system. Whenever excess wind energy is available, the excess electricity generated feeds an electrolyzer which decomposes water into hydrogen and oxygen. The hydrogen produced is then stored and utilized for the production of electricity for domestic customers using fuel cells and hydrogen combustion engines during unavailability of wind energy to produce electricity [10]. An in-depth investigation has been made herein to study the biomass FC-based distributed generation system for sustainable development in Sagar Island.

## 2. Biomass energy resources, scope and prospects for generation of electricity in Sagar Island

Normally, wood, manure and crop residues constitute a major share of biomass resources which consume energy from the sun and then store it using photosynthesis. It is released during burning. Human or animal manure also contains some energy which is not utilized during the normal digestion process. In Sagar Island, abundant solar energy is available throughout the year and due to availability of monsoon water, the production of energy crops and weed-related biomass increases. The forest may be another source of biomass as the island forms part of the largest deltaic complex of the Sundarban area where beside human habitats natural forest exists, supplying adequate forest-related biomass. Along with forest-related biomass, the end product of cultivated crops produces a huge amount of biomass. Dried paddy, mustard and unused betel leaf and plant constitute major biomass sources at Sagar Island. The other major occupations on the island are cattle farming and poultry farming. Therefore, a huge quantity of animal manure is available and can be used as a source of biomass. In the small-scale industries of rice mills, agro-processing industries and molasses production, the production units produce extracts from food grain and from the sugar cane, which also act as sources of biomass. On the other hand, the waste material produced by human daily existence, unused rotten food, waste from the preparation of food as well as waste produced in the Haat Bazaar also generate biomass. Hence, the availability of biomass is huge on Sagar Island, and it may be utilized to generate electricity for the sustainable development of that area.

Biomass energy can be utilized to produce electrical energy by burning the biomass using a gas turbine or steam turbine. But due to low energy density, it is very difficult to transport biomass to a concentrated power plant for burning and utilizing the energy. Storage of biomass for future energy demand is very difficult due to large area requirements and proper protection to maintain quality due to moisture and seasonal temperature variances. But the main problem related to biomass gasification is the environmental issue. Sagar Island has a very sensitive ecosystem. As the burning process introduces hazardous elements and creates environmental pollution, direct burning of biomass is not suitable for Sagar Island. In this situation, hydrogen production from biomass reduces the difficulties related to transportation of biomass as well as the storage difficulties, and protects our environment against hazardous waste. Once hydrogen is produced from the biomass, it is very easy to transport to a different location of the plant and directly store it in a tank for future use.

## 3. Proposed system for generating electricity from biomass

Figure 1 shows the proposed system configuration where the different types of biomass energy are converted into hydrogen. The production of hydrogen from different biomass types is different. Adequate knowledge is required to sectionalize the entire biomass available and direct it to the proper hydrogen production unit. Once hydrogen is produced from the different processes, it is filtered using some scientific processes and stored in a hydrogen storage tank with a suitable form. The hydrogen

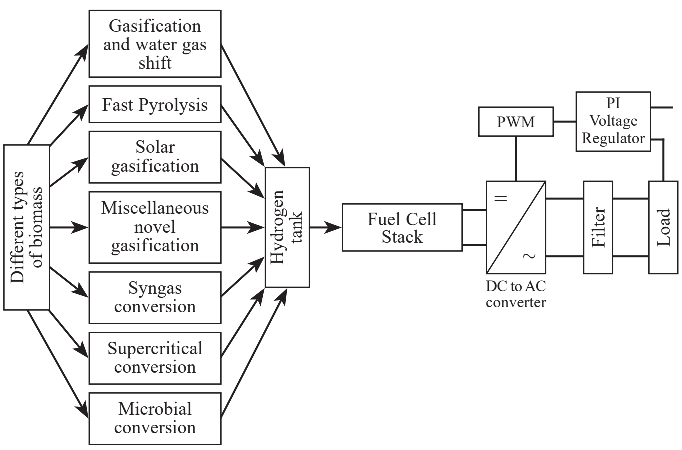


Fig. 1. Layout diagram of biomass based fuel cell power supply system

produced is then sent to the PEMFC, which combines the hydrogen with the oxygen from the air and generates electricity and water. The electricity generated from the fuel cell is DC in nature, and it is further converted into AC using a three-phase inverter. To maintain the desired constant voltage level at the load side, the inverter pulses vary using controller and PWM technology. The quality of the power at the load end also follows the IEEE 519–1992 standard, using a simple LC filter.

**3.1. Hydrogen production from biomass**. The production of hydrogen from different biomasses is possible using different processes, which can be broadly classified as follows [11–15]:
1. Thermo-chemical gasification coupled with water gas shift.
2. Fast pyrolysis followed by reforming of carbohydrate fractions of bio-oil.
3. Direct solar gasification.
4. Miscellaneous novel gasification processes.
5. Biomass-derived syngas conversion.
6. Supercritical conversion of biomass.
7. Microbial conversion of biomass.

**3.1.1. Thermo-chemical gasification coupled with water gas shift**. It is the most common process of hydrogen production from biomass [11, 13]. In this process, the biomass (feedstock includes agricultural and forest product residues of hardwood, softwood and herbaceous species) is heated (under high-rate pyrolysis) to around 600–1000°C in a fluidized bed gasifier and the chemical reaction shown in (1) occurs.

$$\text{Biomass} + O_2 \rightarrow CO + H_2 + CO_2 + \text{Energy} \tag{1}$$

On the other side, gasification is done by bubbling the fluid beds and the high-pressure high-temperature slurry-fed entrained flow gasifier. In all the gasifier reactions a lot of tar and other impurities are generated. They are removed by means of filters and the byproduct CO should be converted into hydrogen by the water gas shift reaction, as shown in (2).

$$CO + H_2O \rightarrow CO_2 + H_2 \tag{2}$$

**3.1.2. Fast pyrolysis followed by reforming of carbohydrate fractions of bio-oil**. Fast pyrolysis is an endothermic process of hydrogen production. At the first stage, biomass is converted into a liquid bio-oil, which is further converted into hydrogen [12, 14]. The production of bio-oil from biomass is shown in (3).

$$\text{Biomass} + \text{Energy} \rightarrow \text{Bio-oil} + \text{Char} + \text{Gas} \tag{3}$$

Once biomass is converted into bio-oil, it is further converted into hydrogen by means of a shift reaction. At the temperature of 750–850°C over a nickel-based catalyst, the bio-oil is converted into hydrogen. The first step in pyrolysis is to use heat to dissociate complex molecules into simple units. Next, the reactive vapors which are generated during the first step are converted into hydrogen. Corresponding reactions are as shown in (4), (5) and (6).

$$\text{Bio-oil} + H_2O \rightarrow CO + H_2 \tag{4}$$

$$CO + H_2O \rightarrow CO_2 + H_2 \tag{5}$$

$$CH1._9O_0{\cdot}_7 + 1.26\,H_2O \rightarrow CO_2 + 2.21\,H_2 \tag{6}$$

Solar energy is also utilized for the gasification of organic solid waste to produce hydrogen. The carbonaceous materials using solar gasification are converted into the syngas quality intermediate product, which is further converted into hydrogen. Normally, a parabolic mirror reflector or a palladium diaphragm is used to obtain the maximum amount of solar energy for such gasification.

**3.1.3. Miscellaneous novel gasification processes**. There are many alternative methods of producing hydrogen from the waste material [13]. Thermonuclear devices are also utilized for the production of hydrogen by vaporizing waste organic materials underground for large-scale hydrogen production purposes. On the other hand, some carbonaceous materials are also converted into hydrogen in just a few steps. Here, the mixture of coal, lime and water was converted into hydrogen in the following manner:

$$In_2O_3 + C \rightarrow In_2O + CO_2 \quad T > 873\text{ K} \tag{7}$$

$$\text{Or,} \quad In_2O_3 + 2C \rightarrow In_2O + 2CO \quad T > 873\text{ K} \tag{8}$$

$$In_2O + 2H_2O \rightarrow In_2O_3 + 2H_2 \quad T > 673\text{ K} \tag{9}$$

Overall stoichiometry gives a maximum yield of 0.172 g $H_2$/g of bio-oil (11.2% based on wood).

**3.1.4. Direct solar gasification**. Using nuclear heat and the carbon cycle, hydrogen gas is produced by means of decomposition of water. As municipal waste contains carbon, it is also utilized to convert the hydrogen [12, 13]. Coal and other forms of solid carbonaceous materials are also utilized for generating hydrogen by oxidizing the carbon into oxides of carbon using the electrochemical process, where the hydrogen is produced at the cathode.

**3.1.5. Biomass-derived syngas conversion**. The simplest process to store the energy of synthesis gas is the sponge-iron process (or steam-iron process) [12]. The synthesis gas is nothing but a mixture of CO and $H_2$ which is further converted into pure hydrogen. The reaction within the sponge-iron process is as follows:

$$\begin{array}{l} Fe_3O_4 + 4CO \rightarrow 3Fe + 4CO_2 \\ (\text{coal, biomass or natural gas}) \end{array} \tag{10}$$

$$3Fe + 4H_2O \rightarrow Fe_3O_4 + 4H_2 \tag{11}$$

The same process is utilized to produce pure hydrogen from reduction gas as well as producer gas.

**3.1.6. Supercritical conversion of biomass**. The total conversion of hydrogen from biomass is possible using a supercritical conversion process [12]. Here, biomass is converted into hydrogen at a lower temperature as compared to the other process with a very high pressure. Biomass is totally converted into hydrogen and no solid residue or char is produced at the end of the reaction. Normally, the temperature and pressure of the hydrogen production processes is higher than the critical pressure and the temperature of water (374°C, 22 MPa), which is further dependent on the type and quality of biomass. For a complete and fast reaction, a flow reactor normally used with carbon-based catalysts, is used to convert almost all types of biomass into hydrogen. The temperature and pressure for the production of hydrogen from different types of biomass are dependent on the different types of biomass mixture and the type of biomass itself (e.g. solid, liquid) and the particle size of the materials, etc.

**3.1.7. Microbial conversion of biomass**. Waste concentrated with a high amount of organic material is one of the prime resources of biomass [12, 14]. The biomass from wastewater should be converted into hydrogen by exploiting it using microbial conversion. The carbohydrate types of substrates are fermented by a consortium of bacteria and converted into hydrogen and carbon dioxide. To produce biohydrogen from waste, *R. sphaeroides RV*, *R. rubrum* and *R. capsulatus* are normally used as they are known to produce hydrogen from such source.

**3.2. Hydrogen storage tank**. Once the hydrogen is produced from the different types of biomass and using different hydrogen production units, it is filtered and stored in a hydrogen storage tank. There are different methods of storing hydrogen. The simplest method of hydrogen storing is in gaseous form using a steel tank, which requires a huge area to store a small amount of hydrogen. However, with the application of new material science technologies, liquid form of hydrogen can be stored using cryogenic liquid hydrogen (critical pressure is 13 bar and critical temperature is –240°C) in a tank with a density of 70.8 $kg/m^3$ at the normal boiling point (–253°C)[16]. The stored hydrogen can be utilized directly to produce electricity or it can be transported to the nearby plant to generate electricity, if required. Other technologies for storing hydrogen gas include chemical storage, solid state storage, underground storage, etc. Problems related to hydrogen storage techniques encompass maintaining the required pressure with minimum space, leakage problems, higher operating and capital cost, high time consumption for storage, and keeping it safe without any loss with minimum maintenance[17]. Liquid hydrogen storage is preferable for transporting fuel to another location but the process entails high costs. For large quantities of gas or long-term storage, underground systems are preferable because of higher safety, low operation and maintenance cost. This is preferable for the proposed study. The underground system performance is impressive as far as safety issues are concerned. As hydrogen has the widest explosive/ignition mix range, any kind of hydrogen leak leads to an explosion when a spark or flame ignites the mixture. In the case of an underground system, the container is isolated from the outside. This means that hydrogen is not ignited if a small amount is leaked from the storage. For even better safety, a micro-fabricated point-contact hydrogen sensor may be used with the storage device to detect any hydrogen leakage and also to resolve the problem before the occurrence of any hazards [9].

**3.3. Fuel cell technology in generating electricity from hydrogen**. The mathematical model of a FC (fuel cell) depends on the electrical and thermal model [18–20]. The combination of these two models describes the dynamics and steady-state behavior of the FC. Figure 2 presents the mathematical model of a PEMFC based on electrical characteristics of the fuel cell.

Based on the electrochemical reaction occurring at the anode and the cathode of a PEM fuel cell, the thermodynamic laws are applied to obtain the mathematical equation and further applied to the Nernst equation to obtain reversible voltage:

$$V_{rev} = 1.229 - 8.45\times10^{-4}\big((T+273.15)-298.15\big) + \\ + 4.31\times10^{5}\big(T+273.15\big)\ln\left(p_{H_2}\sqrt{p_{o_2}}\right) \tag{12}$$

where $T$ is the cell operating temperature in °C. To increase the operating voltage, many cells are stacked together. For the PEMFC stack comprising an $N_s$ number of series-connected cells, the reversible voltage ($V_{rev}$) is obtained by means of (13).

$$V_{rev,\,s} = N_s V_{rev} \tag{13}$$

Reversible voltage of the fuel cell stack has an impact on temperature (T) due to the chemical reaction and the partial pressure of the reactant gases ($P_{H2}$ and $P_{O2}$), as indicated in (1) and (2). The experimental variation of $P_{H2}$ is due to current flows through the fuel cell ($i_{FC}$), as indicated in (14):

$$P_{H_2} = P_0 + P_1 i_{FC} \tag{14}$$

where $P_0$ and $P_1$ are empirical parameters.

**3.3.1. Actual performance.** Actual cell potential is decreased from its ideal potential due to irreversible losses originating primarily from three sources:

1) Activation polarization ($V_{act}$);

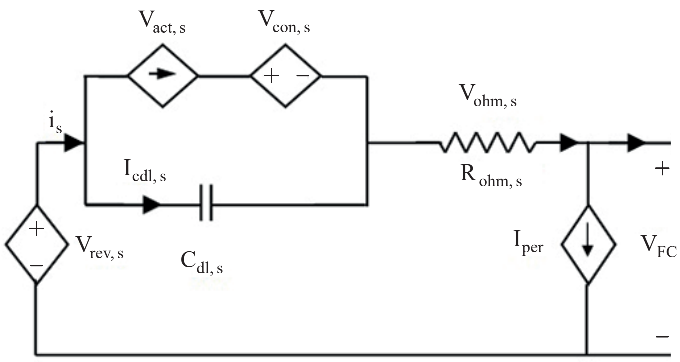


Fig. 2. Fuel cell equivalent circuit

2) Concentration polarization ($V_{conc}$);
3) Ohmic polarization ($V_{ohm}$).

**3.3.1.1. Activation polarization**. Activation polarization deals directly with the rate of electrochemical reactions which have taken place at the FC electrode. The losses are controlled by sluggish electrode kinetics. Mathematical calculation of activation polarization is done using (15) [18, 19]:

$$V_{act} = \frac{RT}{\alpha nF} \ln\left(\frac{i_{act}}{i_0}\right) \tag{15}$$

where n is the number of electrons transferred, R is the ideal gas constant, F is Faraday's constant, $\alpha$ is the charge transfer coefficient, $i_0$ is the exchange current and $i_{act}$ is the activation current passing through the cell. Considering $\alpha$ and $i_0$ as unknown quantities, $v_{act}$ can be experimentally determined from the following equation which is generalized from (15):

$$V_{act} = a + b \ln i_{act}. \tag{16}$$

Considering the temperature effect on the parameter, the expression becomes:

$$a = a_0 + a_1(T + 273.15) \tag{17}$$

$$b = b_0 + b_1(T + 273.15). \tag{18}$$

The FC activation voltage ($v_{act,\,s}$) is obtained for an $N_s$ number series-connected cells as:

$$V_{act}, s = N_s\left[a + b \ln i_{act,s}\right]. \tag{19}$$

Here, the current of the equivalent circuits is:

$$i_{act,s} = \exp\left(\frac{\frac{V_{act}}{N_s} - a}{b}\right). \tag{20}$$

The activation polarization loss is dominant at low current density. In this situation, the electronic barriers must be overcome by the prior to current and ion flow. Activation losses increase as current increases.

**3.3.1.2. Concentration polarization.** Concentration polarization takes place due to the mass transportation into the FC [18–19]. Convection and diffusion phenomena are the reason behind the mass transportation. Among these two, the diffusion phenomena are more dominant as part of transportation of the masses. The convection processes describe the transport of species by the bulk movement of a fluid where the diffusion is the transport of species due to concentration gradients. Because of high current density in the FC, activation polarization is negligible in comparison with concentration polarization, and indicated as:

$$V_{con} = m \exp(ni_{con}) \tag{21}$$

where m and n are empirical parameters.

To obtain the concentration phenomenon for an $N_s$ number of series-connected cells, the equation is modified to:

$$V_{con,s} = N_s\left[m \exp(ni_{con})\right]. \tag{22}$$

To incorporate the temperature effect into the empirical parameter, the relation between the empirical parameters is indicated as:

$$m = m_0 + m_1(T + 273.15) \tag{23}$$

where the other empirical parameter is independent of temperature.

**3.3.1.3. Ohmic polarization**. The flow of ions in the electrolyte introduces Ohmic losses [18, 19]. Ohmic losses may be reduced by decreasing the electrode separation and enhancing the ionic conductivity of the electrolyte. As the electrolyte and fuel cell electrodes obey Ohm's law, Ohmic losses can be expressed by (24):

$$V_{ohm} = R_{ohm} i_{ohm} \tag{24}$$

where $i_{ohm}$ is the current flowing through the cell, and $R_{ohm}$ is the total cell resistance, which includes electronic, ionic and contact resistance.

The FC Ohmic losses and Ohmic resistance are determined as follows for an $N_S$ number of series-connected cells:

$$V_{ohm,S} = N_S R_{ohm} i_S \tag{25}$$

$$R_{ohm,S} = N_S R_{ohm}. \tag{26}$$

Considering the temperature effect on the Ohmic phenomenon:

$$R_{ohm} = R_{ohm,0} + R_{ohm,1}(T + 273.15). \tag{27}$$

**3.3.1.4. Double layer phenomena**. The double layer phenomena are the capacitive effects at the electrode-electrolyte interfaces in each cell due to the transfer (oxidation) and capture (reduction) of electrons [19, 20]. The effect is similar to the performance of an RC network. The network consists of a capacitor ($C_{dl}$), termed as a double layer capacitor, which signifies the accumulation of ionic and electronic charges, and the resistor known as the double layer resistor. For an $N_s$ number of the cells to be connected to the fuel cell, the double layer capacitor ($C_{dl}$, s) is obtained from the fuel cell double layer capacitor ($C_{dl}$) through (28):

$$C_{dl,S} = \frac{C_{dl}}{N_S}. \tag{28}$$

The electrical modeling of the FC double layer effect is based on a capacitor ($C_{dl,\,s}$), as shown in Fig. **2.** This capacitor is connected in parallel to the series connection of the current source and voltage source, representing the activation and concentration phenomena, respectively.

**3.3.2. Peripheral energy consumption**. In the case of the FC, some of the generated energy is consumed by the peripheral circuit [19–20]. The peripheral circuit is modeled as a current source connected in parallel with the FC stack which is shown in Fig. 2. The equation for the current source modeling the FC peripherals, which concerns the FC current ($i_{\mathrm{FC}}$) and the peripherals current ($i_{\mathrm{per}}$), is as follows:

$$i_{per} = k_2 i_{\mathrm{FC}}^2 + k_1 i_{\mathrm{FC}} + k_0. \tag{29}$$

**3.4. Three phase inverter**. A three phase bridge type voltage source inverter (VSI) is implemented to convert generated DC voltage to AC with the desired frequency [21, 22]. Figure 3 shows the circuit diagram of a three phase PWM inverter. The inverter consists of an input capacitor C, which stabilizes the input DC voltage generated by FC. The three legs of the inverter circuit consist of two MOSFET switches, operated by specially designed PWM signals.

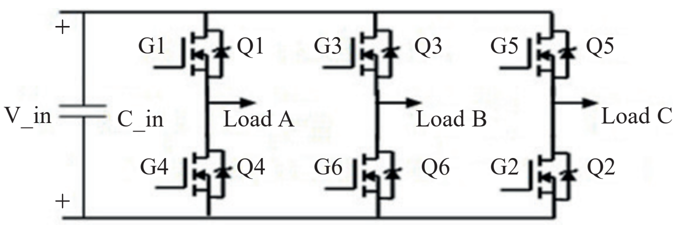

Fig. 3. Three phase inverter circuit

Switches Q1 to Q6 are switched ON and OFF using the desired pulses obtained from a pulse width modulation technique to generate balanced three phase output voltages: $V_{AB}$, $V_{BC}$, and $V_{CA}$, respectively, and to supply a three phase load. The PWM technique consists of three sinusoidal modulating signals with an appropriate phase shift of 120°. Those are generated by the vector control circuit. The signal is compared with a high-frequency triangular carrier signal and it generates the required pulses for switching operation.

The converted voltage of the inverter of the first leg is as follows:

$$(V_{AN})_1 = m_a \frac{V_d}{2} \sin\omega_1 t \tag{30}$$

$$(\hat{V}_{AN})_1 = m_a \frac{V_d}{2}. \tag{31}$$

Therefore, the line-to-line RMS voltage at the fundamental frequency, due to the 120° phase displacement between phase voltages can be written down as:

$$\hat{V}_{LL1} = m_a \frac{\sqrt{3}}{\sqrt{2}} (\hat{V}_{AN})_1 = \frac{\sqrt{3}}{2\sqrt{2}} m_a V_d \tag{32}$$

$$V_{LL1} = \frac{\sqrt{3}}{2\sqrt{2}} m_a V_d \sin\omega_1 t. \tag{33}$$

where $m_a$ is the amplitude modulation supplied by the PID controller vector control unit to control the amplitude of the sinusoidal signal. To control the harmonics quantity, the desired factor is the frequency modulation ratio $m_f$, which is defined as:

$$m_f = \frac{f_s}{f_1} \tag{34}$$

where $f_s$ is the switching frequency and $f_1$ is the fundamental frequency of the inverter. To reduce the harmonics generated due to the switching operation, the $m_f$ should be high enough.

**3.4.1. Inverter controlled pulse generator circuit**. To obtain output voltage at the desired value, a regulator is attached to the system, as indicated in Fig. 4.

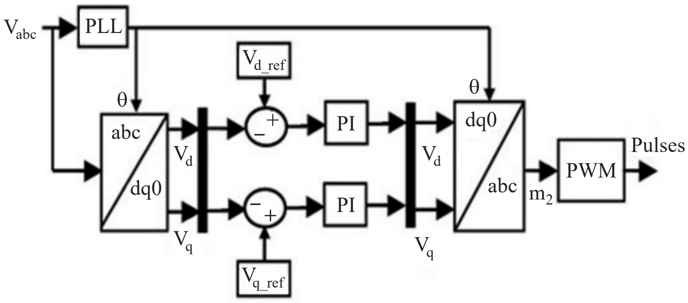

Fig. 4. Block diagram for PI voltage regulator

The regulator generates a control signal to the PWM unit to generate the pulse desired to operate the inverter. To generate the desired control signal, the voltage signal is transformed into a synchronous rotation frame. The generated direct and quadrature component of voltage is further modified using the PI controller to obtain desired voltage and frequency with the help of a phase lock loop (PLL) [23, 24].

## 4. Result and discussion

To obtain the performance of the proposed system, a simulation model of 50 kW, 625 V FC systems has been designed using Matlab/Simulink, and operation of the overall system was observed. The hydrogen generated from the biomass is stored in a hydrogen storage device and supplied to the FC to generate electricity. The FC stack is connected to the three phase inverter to convert the generated DC into desired AC with the desired power quality. The simulation time taken in this analysis is 0.3 second, under which up to 0.1 second, 32 kW, 400 V, 50 Hz, 0.95 PF inductive load (Load 1) is connected. After 0.1 second, two inductive loads 8 kW, 400 V, 50 Hz, 0.9 PF (Load 2) and 8 kW, 400 V, 50 Hz, 0.85 PF (Load 3) are added to the FC stack. After 0.2 second, inductive Load 3 is removed and operation of the whole system is observed.

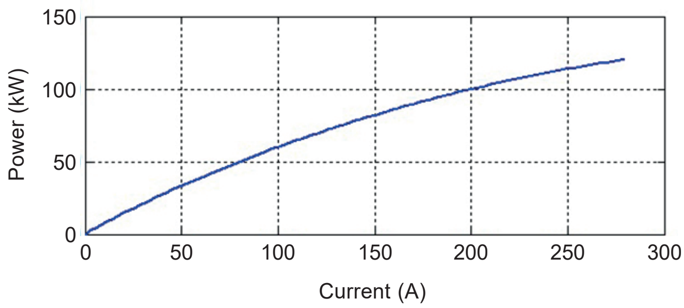


Fig. 5. Fuel cell stack power vs current profile

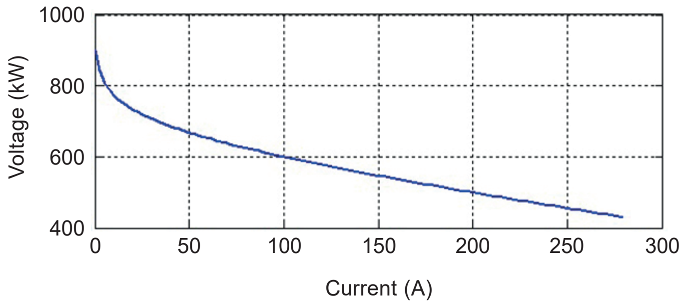


Fig. 6. Fuel cell stack voltage vs current profile

Figure 5 indicates the FC stack power vs the current profile. The power generated maintains an almost proportional relation with the current. The optimum power condition for the current is 80 A.

Figure 6 indicates the FC stack voltage vs the current profile. The voltage generated under the no-load condition is very high and reduces drastically due to load variation. At the optimum power condition, it indicates that the voltage is 625 V.

Figure 7a indicates the operating voltage and Fig. 7b denotes the current profile of the FC stack under variable load conditions. Initially, the voltage obtained from the FC stack oscillates for a short time of 0.003 seconds, and it gradually increases and stabilizes to the optimum voltage around 625 V.

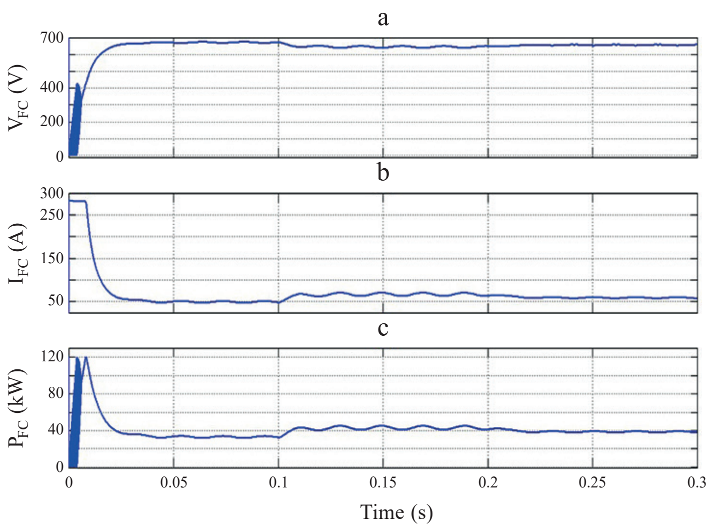


Fig. 7. Fuel cell output voltage, current and power

The change in the connected load varies the voltage around 1.3% of the optimum voltage, which has very little impact on the change in output voltage. The FC stack current profile decreases drastically at the initial stage, from 280 A to 66 A within 0.003 second, and varies due to changes in the connected load at 0.1 and 0.2 second. The power profile indicated by Fig. 7c oscillates for 0.003 second and stabilizes for the entire simulated time based on the connected load.

Figure 8a indicates the input voltage of the inverter and Fig. 8b indicates the voltage profile of the inverter without a filter. Due to the input side filter (LC filter), the initial oscillation is removed and the quality of input voltage to the inverter improves. Once the voltage stabilizes, then due to the change in connected load, a little voltage variation is observed in the input voltage side of the inverter.

Figure 9a indicates the profile of the active power and Fig. 9b indicates the reactive power component of the load.

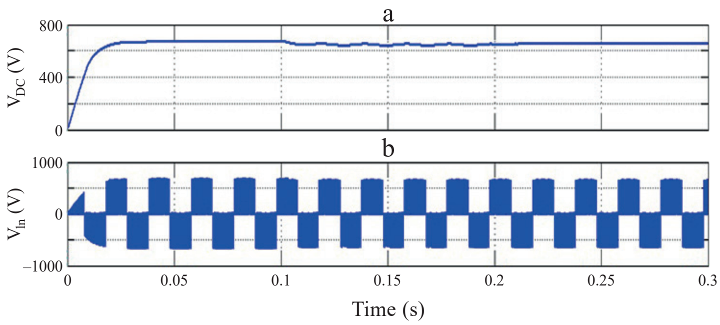


Fig. 8. Inverter input and output voltage

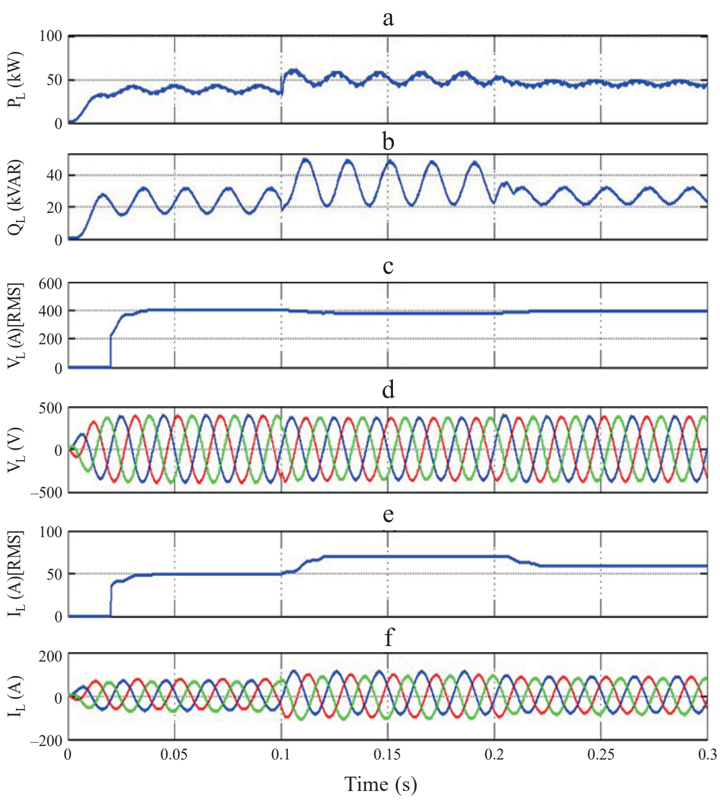


Fig. 9. Load, voltage and current. Active and reactive power profile

Due to the change in the load, both the active and reactive power changes. Figure 9c indicates the three phase RMS load voltage profile of the FC. The RMS value of the voltage profile is constant around 400 V, which is almost constant except for the initial 0.004 seconds. After the initial condition, the voltage profile is almost constant and varies only by 2% due to changes in the load. The change in the load is indicated by the active and reactive power consumption profile. Figure 9d indicates the three phase voltage profile of the connected load which is sinusoidal in nature due to the filter connected to the inverter. Figure 9e indicates the RMS magnitude of the current profile and Fig. 9f indicates the original sinusoidal three phase current profile. Like the voltage profile, the current quantity also stabilized within 0.004 second and increases or decreases within 0.02 second due to changes in the load quantity.

Figure 10 indicates the total harmonic distortion (THD) of the three phase load voltage and Fig. 11 indicates the THD of the load current of the proposed system. Harmonic generation of the system is around 1.93% for voltage and 1.83 % for current quantity, which is lower, as per the IEEE 512–1992 standard. Moreover, the quality of the power obtained using a simple three phase LC filter increases the acceptability of the proposed system.

## 5. Cost analysis of the different distributed generation systems

Based on the local resources and the initial setup cost, the biomass-based gas turbine power supply system and the diesel generator based power supply system are the preferred distributed generation systems other than the proposed method. To calculate the per unit generation cost of the three different power supply systems, the Levelized Cost of Energy (LCOE) method is applied to the different power supply systems and the per unit generation costs are compared. To calculate the per unit cost using the LCOE method, the overnight cost, the discount rate that captures the cost of financing during a specified year, annual fixed and variable operation and maintenance costs and the generation costs are analyzed to estimate the per unit generation cost for a particular power supply system. Further estimation of the generation cost for an individual power supply system is done using (35) [25–26].

$$\text{LCOE} = \text{Overnight cost} + \text{FOM} + \text{VOM} + \text{Generation cost}. \tag{35}$$

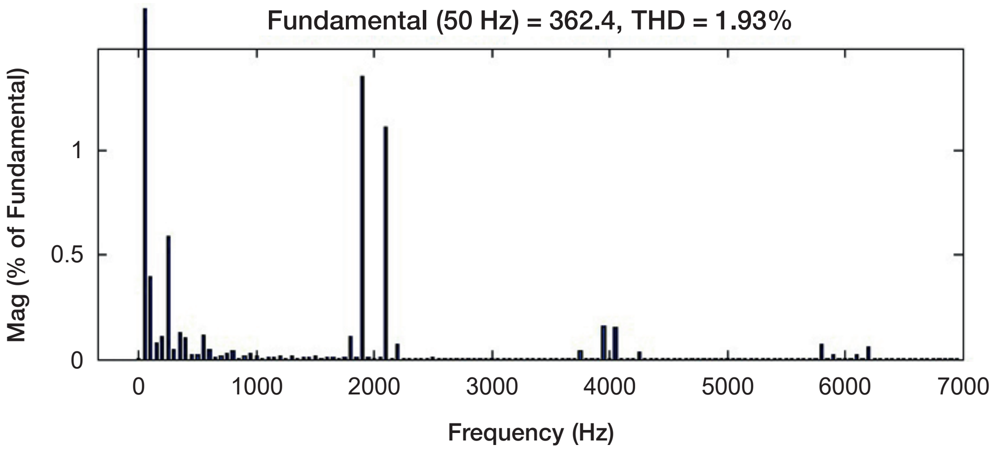


Fig. 10. Voltage quality of the proposed system

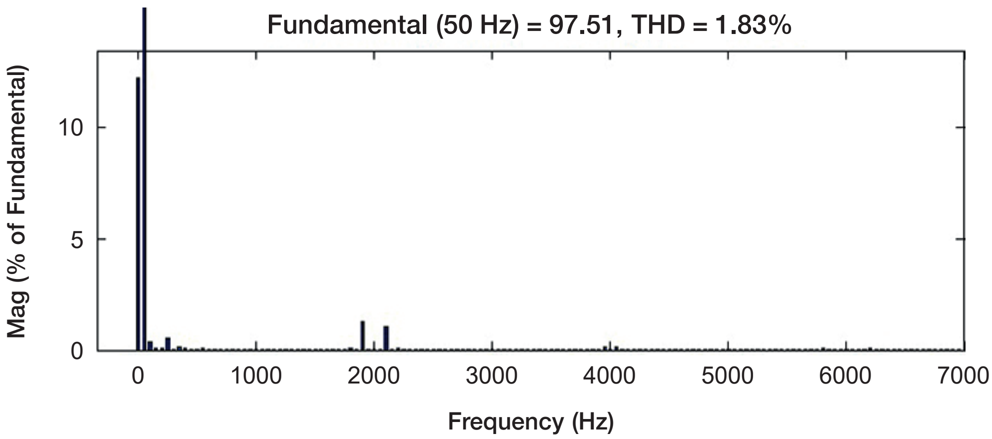


Fig. 11. Current quality of the proposed system

To calculate the annual fixed and variable operation and maintenance costs, the capital recovery factor (CRF) is calculated using the overnight capital cost which has been indicated in (36).

$$CRF = \frac{r(1-r)^i}{(1-r)^{-i}-1} \tag{36}$$

where CRF = Capital Recovery Factor, r is the rate of interest of the weighted average cost of capital (WACC) (11% has been assumed for the proposed case study), i is the investment life (normally the life cycle of the power supply system), FOM: annual fixed operation and maintenance cost and VOM: variable operation and maintenance cost.

The cost comparisons of the three different power plants with the same 50 kW nominal capacities are as follows:

Table 1
Generation costs calculated per unit for the different distributed generation systems

| Sl. No. | Technology | Overnight cost ($) | Per Unit Generation Cost ($/kWh) |
|---|---|---|---|
| 1 | Biomass Gasified | 216850 | 0.1242 |
| 2 | Diesel Generator | 30000 | 0.2351 |
| 3 | Fuel cell | 378100 | 0.1626 |

It is more realistic and more appropriate to estimate the per unit generation cost for a particular area using the Society's Cost of Electricity (SCOE). In the case of SCOE, the environmental and social benefit is included in the per unit generation to evaluate the generation cost and the impact of the power generation on society [27, 28]

$$\begin{aligned} \text{SCOE} = \text{LCOE} &+ \text{cost of climate change damage} + \\ &+ \text{cost of air pollution damage} + \\ &+ \text{system integration costs}. \end{aligned} \tag{37}$$

The calculation of SCOE is based on the available data and the detailed experiment related to the environmental effect. Based on the available data, the different air pollutants are estimated during the generation of electricity using only the three distributed generation systems.

Table 2
Estimated air pollution during generation of electricity

| Sl. No. | Technology | $NO_X$ (lb/MMBtu) | $SO_X$ (lb/MMBtu) | $CO_2$ (lb/MMBtu) | PM (lb/MMBtu) |
|---|---|---|---|---|---|
| 1 | Biomass gasified | 0.08 | 0 | 195 | 0.033 |
| 2 | Diesel generator | 4.41 | 0.29 | 161.4 | 0.62 |
| 3 | Fuel cell | 0 | 0 | 0 | 0 |

Besides the above-listed pollutants, some volatile organic compounds (VOC) are generated for the diesel generator. Moreover, carbon monoxides (CO) have also been generated during operation of both of the systems. Generation of the pollutant component may also change due to the loading effect, engine operating time, aging factor and quality of the fuel. For the biomass gasifier, the generation of pollutant gases depends on the biomass quality and the environmental conditions on the spot where biomass is burned. For the fuel cell power plant, no generation of such pollutant gases occurs during operation. Only a small amount of pollutant gases is generated during the production of hydrogen from different types of biomass. For the distributed generation system, a diesel power plant is a good choice due to lower initial cost, lower starting time, smaller size, simple operation, less setup time and smaller space requirements. Yet the cost per unit of generated electricity is high. For remote areas, the fuel cost increases even further, which causes an increase in the generation costs. Besides the per unit energy cost, the environmental effect is very predominant on Sagar Island. As the diesel generator emits harmful gases, the generation of electricity has an immeasurable effect on the island's environment and it also damages the balance between biodiversity and ecology. The generation of electricity based on biomass is a different choice, based on the availability of biomass on Sagar Island. The generation cost of the biomass power plant is the lowest one, but to maintain biomass quality, huge space is required, which directly affects the cost of generation. Besides the space requirement, the monsoon also plays an important role in the weather conditions. It affects Sagar Island for more than four months and reduces the sunny days. Due to the damp weather conditions, the quality of biomass decreases, which directly affects the generation of electricity from the biomass gasifier-based power plant. The environmental issue is reduced in the case of a biomass gasifier based power supply system, but not fully eliminated. During the burning process, biomass generates harmful gases, which affects the Sagar Island environment. In the case of a fuel cell based system, the different types of biomass are converted into hydrogen and based on the availability of biomass, the hydrogen is generated and stored in the storage tank. The hydrogen can be stored in a tank for a long time and can be used when it is required. Due to the conversion process of the different biomass to hydrogen, the generation cost is further increased, as calculated earlier. But the social benefit of the proposed method is highly essential for Sagar Island's circumstances. The aforesaid process uses waste material, which directly reduces soil and water pollution. On the other hand, the fuel cell emits only oxygen after generation, which has commercial and social benefits. The oxygen emitted may be purified and supplied to key industries, which slashes the per unit generation cost.

## 6. Conclusion

In this paper, a theoretical and mathematical analysis of the generation of biomass by means of a fuel cell based distributed generation system is analyzed. The theoretical process related to hydrogen production from different types of biomass is discussed. The mathematical model of a fuel cell is analyzed and investigated in Matlab/Simulink model to verify the performance of the fuel cell under variable load conditions. A cost analysis of the different distributed generation systems is successfully compared and obtained. It is noteworthy to say that the fuel cell based distributed generation system for Sagar Island is superior as compared to the other distributed generation systems due to the social benefit aspects.

## References


[1] "Power & Energy, National Portal of India", https://www.india.gov.in/topics/power-energy. (*Accessed on- 10.09.2017*).

[2] K. Narula, B.S. Reddy, and S. Pachauri, "Sustainable energy security for India: an assessment of energy demand sub-system", *Applied Ener*. 186(2), 126–139 (2017).

[3] I. Mitra, Optimum utilization of renewable energy for electrification of small islands in developing countries. Kassel: Kassel Univ. Press, 2009.

[4] R.M. Moharil and P.S. Kulkarni, "A case study of solar photovoltaic power system at Sagardeep Island, India", *Renew. and Sustain. Ener. Reviews*. 13(3),673–681 (2009).

[5] A. Das and V. Balakrishnan, "Sustainable energy future via grid interactive operation of SPV system at isolated remote island", *Renew. and Sustain. Ener. Reviews*. 16(7), 5430–544**2.** (2012).

[6] S. Chakrabarti and S. Chakrabarti, "Rural electrification programme with solar energy in remote region–a case study in an island", *Ener. Policy*. 30(1), 33–42 (2002).

[7] H.E. Lindstad, G.S. Eskeland, and A. Rialland, "Batteries in offshore support vessels – Pollution, climate impact and economics", *Tranp. Resear. Part D: Transport and Envir*. 50, 409–417 (2017).

[8] K. DH, C. M., and O. OA, "Potential environmental and human health impacts of rechargeable lithium batteries in electronic waste", *Envir. Sc. & Tech*. 47(10), 5495–5503 (2013).

[9] W.A. Amos, *Costs of Storing and Transporting Hydrogen*, National Renewable Energy Laboratory, 1999.

[10] Ø. Ulleberg, T. Nakken, and A. Eté, "The wind/hydrogen demonstration system at utsira in norway: evaluation of system performance using operational data and updated hydrogen energy system modeling tools" *Intern. J. of Hydr. Ener*., 35(5), 1841–1852 (2010).

[11] R. Schmersahl, M. Klemm, R. Brunstermann, and R.R. Widmann, "Hydrogen from biomass" *Encyclop. of Sustain. Sc. and Tech*., 5116–5133 (2012).

[12] T.A. Milne, C.C. Elam, and R.J. Evans, *Hydrogen from Biomass State of the Art and Research Challenges*, Report for IEA, IEA/H2/TR-02/001. Golden, CO: National Renewable Energy Laboratory; 2002.

[13] G. Sołowski, M.S. Shalaby, H. Abdallah, A.M. Shaban, and A. Cenian, "Production of hydrogen from biomass and its separation using membrane technology", *Renew. and Sustain. Ener. Reviews*. 82(3), 3152–3167 (2018).

[14] A.Sharma and S.K. Arya, "Hydrogen from algal biomass: A review of production process", *Biotech. Rep. (Amst)*. 15, 63–69 (2017).

[15] H. Balat and E. Kırtay, "Hydrogen from biomass – present scenario and future prospects", *Intern. J. of Hydr. Ener*., 35(14), 7416–7426 (2010).

[16] T. Ohta and T.N. Veziroglu, "Energy carriers and conversion systems with emphasis on hydrogen", V 1. Eolss Publishers Co Ltd, 2009.

[17] T. Sinigaglia, F. Lewiski, M.E.S. Martins, and J.C.M. Siluk, "Production, storage, fuel stations of hydrogen and its utilization in automotive applications – a review", *Intern. J. of Hydr. Ener*., 42(39), 24597–24611 (2017).

[18] C. Spiegel, *PEM Fuel Cell Modeling and Simulation Using Matlab*, Academic Press, Boston, 2008.

[19] I.S. Martín, A. Ursúa, and P. Sanchis, "Modelling of PEM fuel cell performance: Steady-state and dynamic experimental validation", *Energies*, 7(12), 670–700(2014).

[20] M.T. Stocker, B.M. Barnes, M. Sohn, E. Stanfield, and R.M. Silver, "Development of large aperture projection scatterometry for catalyst loading evaluation in proton exchange membrane fuel cells", *J. of Pow. Sourc*., 364,130–137 (2017).

[21] N. Mohan, T.M. Undeland, and W.P. Robbins, *Power Electronics: Converters, Applications, and Design*, Wiley India, 2007.

[22] V. Miichal, "Three-level PWM floating h-bridge sinewave power inverter for high-voltage and high-efficiency applications", *IEEE Trans. on Pow. Electr*., 31(6) 4065–4074 (2016).

[23] M. Bobrowska-Rafal, K. Rafal, M. Jasinski, and M.P. Kazmierkowski, "Grid synchronization and symmetrical components extraction with PLL algorithm for grid connected power electronic converters – a review", *Bull. Pol. Ac.: Tech*. 59(4), 485–497 (2011).

[24] L. Liu and C. Liu, "Deliberations about three-phase PLL technologies applied to a grid control of the renewable power system." *Bull. Pol. Ac.: Tech*. 63(1), 261–267 (2015).

[25] M.Y. Roche, Comparison of Costs of Electricity Generation in Nigeria – Technical Report, Abuja, 2017.

[26] Atavane and P. Vijai, "Managing new energy technology alternatives for india's captive power industry", *ASME Pow. Confc*., 711–721 (2004).

[27] "Annual Energy Outlook – Energy Information Administration", *www.eia.gov/outlooks/aeo/pdf/0383(2016).pdf. (Accessed on 08.12.2017)*.

[28] S. Baurzhan and G.P. Jenkins, "On-grid solar pv versus diesel electricity generation in sub-saharan africa: Economics and GHG emissions", *Sustainability* 9(372), 1–15 (2017).